

Fe(III)-salen encapsulated Al-MCM-41 as a catalyst in the polymerisation of bisphenol-A

Halimaton Hamdan *, Vivin Navijanti, Hadi Nur, Mohd Nazlan Mohd Muhid

Ibnu Sina Institute for Fundamental Science Studies, Universiti Teknologi Malaysia, 81310 UTM Skudai, Johor, Malaysia

Received 6 September 2004; received in revised form 30 September 2004; accepted 10 October 2004

Available online 21 December 2004

Abstract

Fe(III)-salen complexes encapsulated in the channels of Al-MCM-41 molecular sieves were successfully synthesised in situ by the flexible ligand method. The resulting compound was characterised by XRD, IR spectroscopy, nitrogen adsorption isotherm and ¹H NMR techniques. The loading of complexes in Al-MCM-41 depends on the quantity of framework aluminium, suggesting that there is an electrostatic interaction between the positive charges of the encapsulated Fe(III)-salen complexes and the negative charges of the Al-MCM-41 framework. Polymerisation of bisphenol-A catalysed by Fe(III)-salen-Al-MCM-41 gave 67% conversion; significantly higher than the conventional homogeneous Fe(III)-salen catalyst.

© 2004 Elsevier SAS. All rights reserved.

Keywords: Encapsulated Fe(III)-salen-Al-MCM-41; Zeozyme catalyst; Polymerisation; Bisphenol-A

1. Introduction

Metal complexes encapsulated into molecular sieves with suitable pore sizes such as zeolite Y, VPI-5 and mesoporous MCM-41 via covalent or ionic bonding, is expected to be as active as those present in metalloenzyme. Furthermore, the hybrid complex formed is structurally and thermally more stable, remain unchanged during reactions and gives higher conversions [1–3]. A number of metal complexes, for example Cu-phthalocyanine, Cu-salen, Cr-salen, Cu-pyridine, Mn-salen, Pd-salen and V-salen have been synthesised and encapsulated into molecular sieves such as zeolite Y [4–9].

Encapsulation of complexes into zeolite Y offers certain advantages whereby relatively large complexes (0.8 nm) cannot easily move in or out of the zeolite window (0.7 nm) which is smaller in size than the pores (1.2 nm). Unfortunately, reactions are only limited to small substrates since big substrates cannot enter the pores. In order to enable reactions involving bigger substrates, mesoporous MCM-41

having large pore size (2–5 nm) was used as an alternative. However the disadvantage of using MCM-41 as the host molecule is that the encapsulated active complex could easily be leached out. Because of this, some silicon atoms in the framework are substituted with aluminiums in order to induce ionic interactions between the positively charged metal complexes and the negatively charged framework aluminiums.

Although many studies have been reported on the synthesis of zeozymes or hybrid systems, Fe(III)-salen-Al-MCM-41 has not been reported. In this system, Fe(III)-salen complex acts as the guest with the active sites, whereas Al-MCM-41 as the host. Salen, (*N,N'*-bis(salicylidene)-ethylenediamine) being flexible in nature, enables it to easily penetrate the parallel channels of the hexagonal lattice structure of the mesoporous MCM-41. MCM-41 is also capable of protecting the active sites from detrimental reactions, preparing empty spaces for the substrates and active sites to react and directing the formation of bonds in a reaction.

This paper reports an in situ synthesis of Fe(III)-salen complex in the cavities of Al-MCM-41, by the flexible ligand method [10]. The physicochemical properties of the

* Corresponding author.

E-mail address: hali@kimia.fs.utm.my (H. Hamdan).

so-called hybrid complex or zeozyme was characterised by X-ray diffraction (XRD), temperature programmed oxidation (TPO), infrared spectroscopy (IR), nitrogen adsorption isotherm and ^1H NMR techniques. The catalytic activity of the Fe(III)-salen-Al-MCM-41 complex was studied in the oxidative polymerisation of bisphenol-A, using aqueous 30% H_2O_2 as the oxidant at room temperature.

2. Experimental

2.1. Synthesis of Fe(III)-salen-Al-MCM-41

Al-MCM-41 was synthesised directly using established technique [11]. The composition of the gel mixture was based on the ratio: $x\text{Al}_2\text{O}_3:6\text{SiO}_2:\text{HTABr}:1.5\text{Na}_2\text{O}:0.15(\text{N}-\text{H}_4)_2\text{O}:250\text{H}_2\text{O}$ with sodium aluminate (NaAlO_2) as the aluminium source. Four Al-MCM-41 samples with $\text{SiO}_2:\text{Al}_2\text{O}_3$ ratios of 40, 60 and 120 were synthesised following the gel composition listed in Table 1; labelled as AM-40, AM-60 and AM-120, respectively. Salen (*N,N'*-bis(salicylidene)-ethylenediamine) was synthesised by reaction of 1 mol ethylenediamine and 2 mol salicylaldehyde under reflux for 1 h. The yellow salen solid was washed with petroleum ether, dried and characterised. The synthesis of Fe(III)-salen (FS) complex was carried out by mixing 4.02 g (0.015 mmol) salen with 1 g (0.005 mol) iron trichloride anhydrate and 150 mL ethanol. The mixture was refluxed at 100°C for 1 h. The precipitate was filtered, washed and dried and characterised by FTIR. Fe(III)-Al-MCM-41 (FAM) was prepared by exchanging Fe^{3+} cations into Al-MCM-41 [12]. Encapsulation of salen into Fe(III)-Al-MCM-41 to form Fe(III)-salen-Al-MCM-41 (FSAM) was carried out by the flexible ligand technique. 0.007 mol salen was added to 5 g Fe(III)-Al-MCM-41 and stirred at 150°C in an oil bath for 3 h under a nitrogen gas flow. Excess Fe^{3+} ions in the solid were removed by ion exchange with 0.01 M NaCl solution and washing with hot water. Unreacted salen was removed by soxhlet extraction using dichloromethane until the colour of the extract disappeared. The calcined samples were characterised by XRD, FTIR and nitrogen adsorption.

2.2. Polymerisation of bisphenol-A

FSAM catalyst (100 mg) was reacted with bisphenol-A (5.0 mmol) in 10 mL dioxane with dropwise addition of aqueous 3.4 mL 30% H_2O_2 for 3 h at room temperature. The product of the reaction was filtered in order to separate

the catalyst from the solution and the filtrate was directly added into a 100 mL (50:50 v/v) methanol–water mixture. The solid product was centrifuged, dried and characterised. The same procedure was repeated for FS catalyst (3.8 mg).

2.3. Characterisations

Powdered X-ray diffraction (XRD) patterns of samples were recorded at 2θ of 1.5° to 10° on a Siemens D5000 powder diffractometer with $\text{Cu-K}\alpha$ radiation at 35 kV and 35 mA. The BET surface areas and the pore size distributions were measured on a Micromeritics volumetric adsorption analyzer (ASAP 2010). Infrared spectra were recorded on Shimadzu 8000 spectrometer, using the KBr wafer technique. Fe(III)-salen-Al-MCM-41 (FSAM) sample; prepared as self-supporting wafer, was placed in a quartz cell equipped with CaF_2 window, and heated in a tube furnace under vacuum ($p = 1 \times 10^{-8}$ mbar) at 150°C for 5 h. IR spectra of the cooled samples were recorded at the wavenumber range of $1700\text{--}1300\text{ cm}^{-1}$. Temperature programmed oxidation (TPO) data was obtained from Thermoquest TPDRO 1100. Samples were heated to 200°C in a flow of nitrogen gas and analysed by flowing a gas mixture of 7.5% oxygen in helium at a rate of 30 mL min^{-1} from 200 to 600°C . ^{29}Si MAS NMR spectra were recorded on a Bruker 400 MHz Avance at a frequency of 79.5 MHz, spinning at 5.5 kHz using 45° pulses with a relaxation delay of 600 s. ^{13}C and ^1H MAS NMR spectra were recorded at a frequency of 100.6 and 399.9 MHz, spinning at 5 kHz using 1.9 μs pulses at 2 s relaxation time delays.

3. Results and discussion

X-ray diffractograms of SiMCM-41 and H-Al-MCM-41 samples with various $\text{SiO}_2:\text{Al}_2\text{O}_3$ ratios (AM-40, AM-60 and AM-120) in Fig. 1 consist of up to four reflections typical of hexagonal lattice structure of mesoporous MCM-41; indexed as (100), (110), (200), (210), respectively [13]. The appearance of intense peaks reflects the high degree of long range order of the samples. The peaks were broadened and shifted to higher angles with increase in the aluminium content. This means that the interplanar distance increases or there is an increase of the pore diameter of the AlMCM-41 (Fig. 1) since the ionic size of Si^{4+} (0.41 Å) ions are smaller than the Al^{3+} (0.53 Å) ions, which results in shorter Si–O bonds (1.61 Å), compared to Al–O bonds 1.75 Å [14].

Fe(III)-salen-Al-MCM-41 complex was brown in colour. The intensities of peaks in the X-ray diffractograms of Al-MCM-41 samples (Fig. 2) do not show much difference before and after encapsulation of Fe(III)-salen, indicating that the structure of Al-MCM-41 was not affected and remained intact throughout the process. There is a general shift of the peaks towards lower angles for MCM-41 samples having larger aluminium content; suggesting contraction of the pore diameter implying the formation of Fe(III)-salen complex.

Table 1
Composition of mixture

Sample	Al_2O_3	SiO_2	CTA_2O	Na_2O	$(\text{NH}_4)_2\text{O}$	H_2O
AM-40	0.15	6	1	1.5	0.15	250
AM-60	0.10	6	1	1.5	0.15	250
AM-120	0.05	6	1	1.5	0.15	250

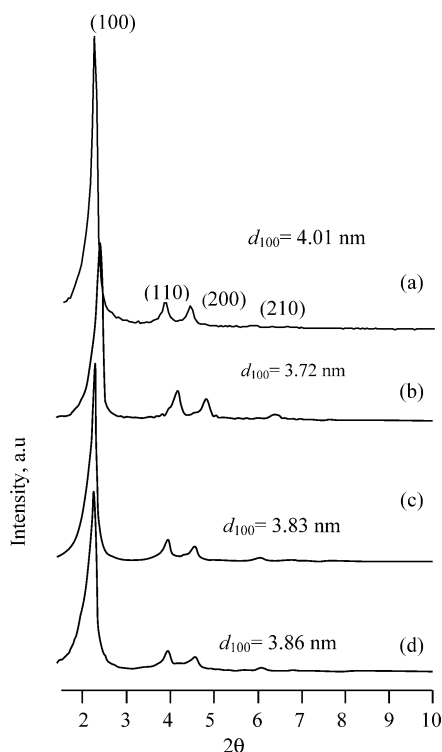


Fig. 1. X-ray diffractograms of (a) SiMCM-41, (b) AM-120, (c) AM-60 and (d) AM-40.

The encapsulation of Fe(III)-salen was further confirmed by X-ray diffraction measurement and infrared spectroscopy (Table 2). Fig. 3 shows the IR spectra of samples FAM-60, FSAM-60, FS and salen after being heated in vacuum at 150 °C. The peaks associated with the CH₂-N bonds of the salen complex are observed at 1700–1300 cm⁻¹ region of the IR spectrum. As expected, sample FAM-60 does not show any peaks in this region. Samples FSAM-60, FS and salen display similar peaks with some variations in position and intensities. There is a general shift of the peaks towards lower wavenumbers for samples FS and FSAM-60 with respect to salen due to two reasons. First, Fe cations are not in a free condition as in Fe-salen complex, instead they are bonded to the Al-MCM-41 framework as a charge neutralizer. Second, the Fe-salen being encapsulated in the channel of Al-MCM-41 restrict the movement of the complex due to lack of space. The presence of similar peaks indicates that

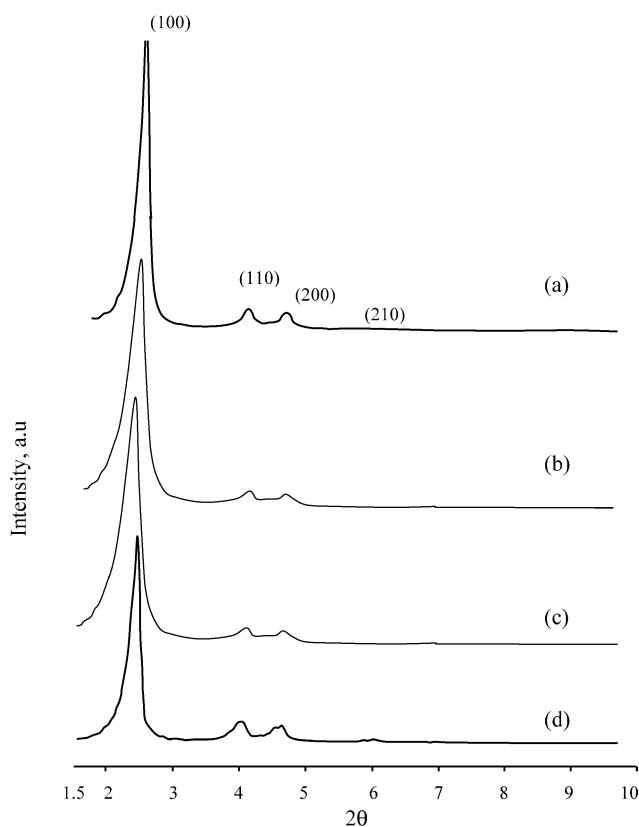


Fig. 2. X-ray diffractograms of (a) FAM-60, (b) FSAM-40, (c) FSAM-60, (d) FSAM-120.

Fe(III)-salen complex has been successfully encapsulated into the Al-MCM-41 framework. There was no substantial leaching of the complex since sample FSAM was exposed to soxhlet extraction with dichloromethane for three days.

Quantitative analysis on Fe(III)-salen in Al-MCM-41 (FSAM) with various SiO₂:Al₂O₃ ratios by IR given in Table 2 generally indicates that a larger quantity of Fe(III)-salen complexes are encapsulated into the Al-MCM-41 framework with lower SiO₂:Al₂O₃ ratios. Therefore, the loading of Fe(III)-salen complexes in Al-MCM-41 is dependent on the quantity of framework aluminium incorporated in MCM-41. The positive charges from the Fe(III)-salen complexes interact electrostatically with the negative charges of the framework Al, causing them to be strongly

Table 2
Characterisation data of Fe(III)-salen-Al-MCM-41 catalysts

Sample	SiO ₂ /Al ₂ O ₃	Pore diameter (nm) ^c	Fe/Al-MCM-41 (wt/wt%)	CH ₂ -N peak area of complexes at 1602 cm ⁻¹ stretching (au) ^a
FSAM-120 ^b	120	3.29	0.62	600
FSAM-60 ^b	60	3.42	0.91	900
FSAM-40 ^b	40	3.46	1.23	1600
FAM-60 ^b	60	3.67	1.27	–

^a Analysed by FTIR.

^b Heterogeneous catalysis.

^c Analysed by XRD.

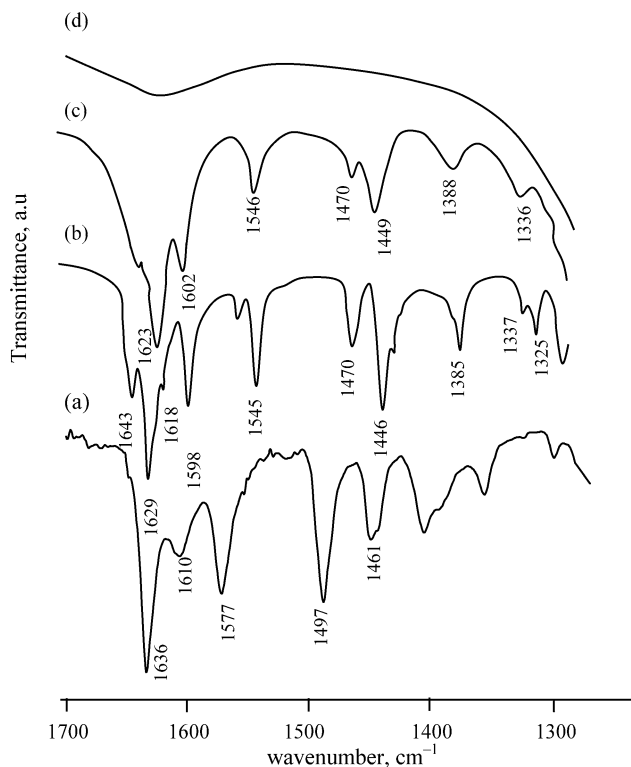


Fig. 3. IR spectra of (a) salen, (b) Fe(III)-salen (FS), (c) Fe(III)-salen-Al-MCM-41 (FSAM-60) and (d) Fe(III)-Al-MCM-41 (FAM-60) after heating in vacuum.

Table 3
Surface properties of Fe(III)-salen-Al-MCM-41 ($\text{SiO}_2/\text{Al}_2\text{O}_3 = 60$)

Sample	$S_{\text{BET-N}_2}$ ($\text{m}^2 \text{g}^{-1}$) ^a	$V_{\text{p-N}_2}$ ($\text{cm}^3 \text{g}^{-1}$) ^b	WBJH-N ₂ (nm) ^c	%Fe (AAS) ^d
FAM-60	979	0.42	2.92	1.27
FSAM-60	670	0.32	2.30	0.91

^a Surface area.

^b Mesopore volume.

^c Pore diameter.

^d Percentage of Fe calculated from AAS.

bonded to the framework and prevent them from being leached out.

The nitrogen adsorption studies of samples FAM-60 and FSAM-60 (Table 3) indicate a decrease in the surface area, pore volume and pore diameter by 31%, 25% and 21%, respectively; further confirms the encapsulation of salen into Fe(III)-Al-MCM-41. The percentage of iron in FSAM is lower than in FAM by about 30%. The reduction suggests that during encapsulation of salen, only iron that became part of the FSAM complex remained unleached in the system.

TPO profiles of samples FSAM with various $\text{SiO}_2/\text{Al}_2\text{O}_3$ ratios in Fig. 4 indicate the presence of peaks of various intensities at 325–400 °C region. The absence of the peak in sample FAM suggests that iron is present as Fe_2O_3 . Whereas the presence of peaks in the region indicates that the amount of gas produced as a result of oxidation of sample is higher than the amount of oxygen needed for the reaction. Quanti-

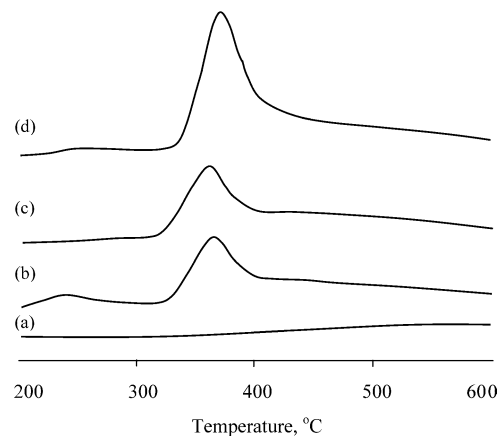
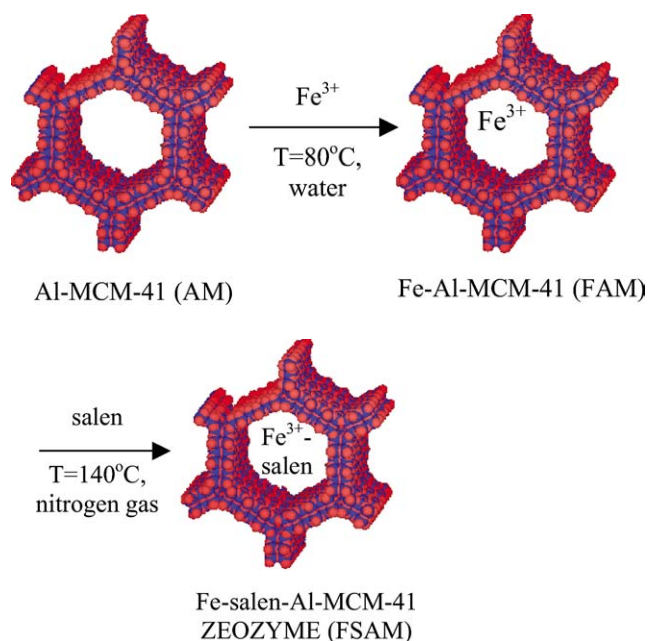


Fig. 4. TPO profiles of (a) FAM-40, (b) FSAM-120, (c) FSAM-60 and (d) FSAM-40.

tative analysis indicates that an increase in the $\text{SiO}_2/\text{Al}_2\text{O}_3$ ratio of the Al-MCM-41 shows a decrease in the intensity of peak due to lower organic content of the gas produced; implying less Fe-salen complex being formed. This results further supports prior observation that a higher amount of salen is encapsulated into the framework with more aluminium.

The diagrammatic representation of the steps involved in the formation of Fe(III)-salen-Al-MCM-41 zeozyme complex is as follows:



The catalytic reactivity of FSAM zeozyme complex was tested in the polymerisation of bisphenol-A with hydrogen peroxide as the oxidising agent and dioxane as the solvent. The test results (Table 4) indicate that the higher the loading of iron complexes, the higher is the conversion of bisphenol-A, with a maximum of 66.7% produced by sample FSAM-40; significantly higher than that produced by homogeneous Fe(III)-salen catalyst. Although the functional groups in bisphenol-A and polybisphenol-A are the same,

Table 4
Catalytic tests on polymerisation of bisphenol-A^a

Catalyst	Quantity of polybisphenol-A (g)	Percentage of reacted bisphenol-A
Fe(III)-salen (FS)	0.22	19.3
FSAM-40	0.76	66.7
FSAM-60	0.71	62.3
FSAM-120	0.38	33.3

^a All reactions were carried out at room temperature for 3 h: 100 mg catalyst; 5 mmol bisphenol-A; 3.4 mL 30% H₂O₂; 10 mL dioxane.

Table 5
Physical properties of bisphenol-A and polybisphenol-A

Property	Bisphenol-A	Polybisphenol-A
Colour	White	Brown
Melting point	153 °C	300–320 °C
Solubility (methanol–water)	Soluble	Insoluble

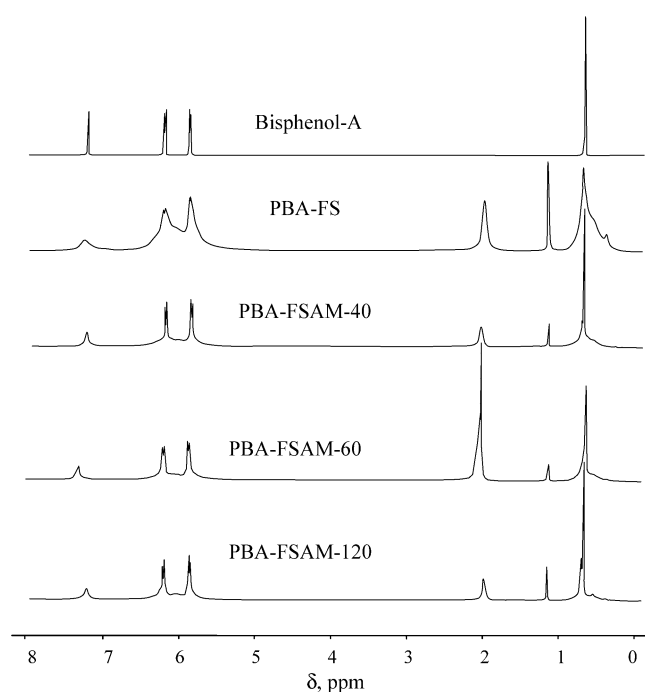


Fig. 5. ¹H NMR spectra of bisphenol-A and polymerisation product polybisphenol-A.

these materials can be distinguished from their physical properties which are significantly different as listed in Table 5. The activity of the catalyst remained unaffected after it was recycled twice but was found to decrease by more than 50% after the third recycle.

Fig. 5 shows the ¹H NMR spectra of bisphenol-A and the polybisphenol-A produced from various catalytic reactions. Generally, all spectra show four similar peaks: $\delta = 0.8$ ppm for methyl; $\delta = 5.8$ – 6 ppm for aromatic proton in the *ortho* position, $\delta = 6.2$ – 6.4 ppm for aromatic proton at *meta* position and $\delta = 7.2$ for OH groups [15]. The peak at $\delta = 1.3$ and 2 ppm are for acetone. However the spectra for polybisphenol consist of broader peaks due to the presence of

more chemically inequivalent environment; typical of polymeric molecules.

Polymerisation of bisphenol-A is an oxidative polymerisation process. By using zeozyme complexes, the amount of polymer produced is much higher due to the hydrophilic nature of Al-MCM-41 which supports the adsorption of bisphenol-A towards the formation of phenoxy radicals. Bisphenol-A is then oxidised by the oxidant H₂O₂ catalysed by Fe(III)-salen-Al-MCM-41 to form the phenoxy radicals. The last stage of polymerisation is the combination of the radicals to form polybisphenol-A chains.

4. Conclusion

Fe(III)-salen-Al-MCM-41 has been successfully synthesised by the flexible ligand method. The quantity of Fe(III)-salen complexes encapsulated into Al-MCM-41 to form the zeozyme complex is related to the quantity of aluminium in the framework via an electrostatic interaction between the positively charged encapsulated complexes and negatively charged Al-MCM-41 framework. Encapsulation of the Fe(III)-salen into the pore of Al-MCM-41 is supported by a decrease in the pore volume and surface area of the host system. Fe(III)-salen-Al-MCM-41 zeozyme was an active catalyst for polymerisation of bisphenol-A with 100% selectivity and 67% conversion. The decrease in surface area of the catalyst complex supports that the oxidation of bisphenol-A occurred on the active sites of Fe(III)-salen encapsulated in the pores rather than those adsorbed on the external surface of the Al-MCM-41 host molecular sieves.

Acknowledgement

The authors thank the Ministry of Science, Technology and Innovation, Malaysia and Universiti Teknologi Malaysia for funding.

References

- [1] D. Chatterjee, A. Mitra, *Mol. Catal. A: Chem.* 144 (1999) 363–367.
- [2] A. Bottcher, M. Grinstaff, J. Labinger, H. Gray, *Mol. Catal. A: Chem.* 113 (1996) 191–200.
- [3] F.R. Hartley, *Supported Metal Complexes: A New Generation of Catalysts*, Reidel, 1985.
- [4] N. Herron, *CHEMTECH* (1989) 542–548.
- [5] K.J. Balkus Jr., A.K. Khanmamedova, K.M. Dixon, F. Bedioui, *Appl. Catal. A: Gen.* 143 (1996) 159–173.
- [6] R.F. Parton, G.J. Peere, P.E. Neys, P.A. Jacobs, R. Claessens, G.V. Baron, *Mol. Catal. A: Chem.* 113 (1996) 445–454.
- [7] S. Ernst, R. Glaser, M. Selle, *Prog. Zeolite Micropor. Mater.* 105 (1997) 1021–1028.
- [8] S.P. Varkey, C. Ratnasamy, P. Ratnasamy, *Mol. Catal. A: Chem.* (1998) 135.
- [9] S. Nakagaki, C.R. Xavier, A.J. Wosniak, A.S. Mangrich, F. Wypych, M.P. Cantao, I. Denicolo, L.T. Kubota, *Colloids Surf. A: Physicochem. Engrg. Aspects* 168 (2000) 261–276.
- [10] S. Ernst, M. Selle, *Micropor. Mesopor. Mater.* 27 (1999) 355–363.

- [11] J.M. Kim, J.H. Kwak, S. Jun, R. Ryoo, *J. Phys. Chem.* 99 (1995) 16743–16747.
- [12] J. Okamura, S. Nishiyama, S. Tsuruya, M. Masai, *J. Mol. Catal. A: Chem.* 135 (1998) 133–142.
- [13] J.S. Beck, J.C. Vartuli, W.J. Roth, M.E. Leonowicz, C.T. Kresge, K.D. Schmitt, C.T.-W. Chu, D.H. Olson, E.W. Sheppard, S.B. McCullen, J.B. Higgins, J.L. Schlenker, *J. Amer. Chem. Soc.* 114 (1992) 10834–10843.
- [14] X.S. Zhao, G.Q. Lu, G.J. Millar, *Ind. Chem. Res.* 35 (1996) 2075–2090.
- [15] X.G. Li, M.R. Huang, L.X. Wang, M.F. Zhu, A. Menner, J. Springer, *Synth. Met.* 123 (2001) 435–441.